NANO LETTERS
Letter
Cite This: Nano Lett. 2019, 19, 6711−6715
pubs.acs.org/NanoLett

Accurate Mass Measurement of a Levitated Nanomechanical Resonator for Precision Force-Sensing

F. Ricci,*[,†] M. T. Cuairan,[†] G. P. Conangla,[†] A. W. Schell,[†,‡] and R. Quidant*[,†,¶]

[†]ICFO-Institut de Ciencies Fotoniques, The Barcelona Institute of Science and Technology, 08860 Castelldefels, Barcelona, Spain
[‡]Central European Institute of Technology, Brno University of Technology, Purkynova 123, CZ-612 00 Brno, Czech Republic
[¶]ICREA-Institució Catalana de Recerca i Estudis Avançats, 08010 Barcelona, Spain

Supporting Information

ABSTRACT: Nanomechanical resonators are widely operated as force and mass sensors with sensitivities in the zepto-Newton (10^{-21}) and yocto-gram (10^{-24}) regime, respectively. Their accuracy, however, is usually undermined by high uncertainties in the effective mass of the system, whose estimation is a nontrivial task. This critical issue can be addressed in levitodynamics, where the nanoresonator typically consists of a single silica nanoparticle of well-defined mass. Yet, current methods assess the mass of the levitated nanoparticles with uncertainties up to a few tens of percent, therefore preventing to achieve unprecedented sensing performances. Here, we present a novel measurement protocol that uses the electric field from a surrounding plate capacitor to directly drive a charged optically levitated particle in moderate vacuum. The developed technique estimates the mass within a statistical error below 1% and a systematic error of ∼2%, and paves the way toward more reliable sensing and metrology applications of levitodynamics systems.

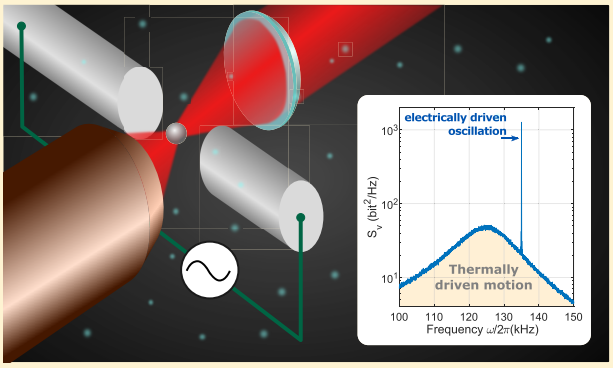

KEYWORDS: *mechanical resonators, optical levitodynamics, levitation optomechanics, force sensing, vacuum*

Nanomechanical resonators play a leading role in the field of force,[1] mass,[2] and charge[3] sensing. Thermal noise represents the ultimate limitation in the their sensitivity,[4,5] and hence, clamped resonators are usually operated in cryogenic environments.[6]

Owing to their unprecedented decoupling from the environment, levitated nanomechanical systems have recently been able to reach room temperature performances comparable to such clamped cryogenic nanoresonators,[7−9] yet with a sensible reduction of the complexity of the apparatus. Moreover, the negligible mechanical stresses introduced by levitation allow to fulfill the rigid body approximation. As a result, the mass of the resonator is uniquely defined by the inertial mass of the levitated nanoparticle and does not require precise assessment of the system's geometry, knowledge on material properties, and complex flexural models for the shape of the oscillation modes, as it is the case for clamped systems.

Despite zepto-Newton resonant force sensitivities with levitated nanoparticles in vacuum have been predicted[10] and demonstrated,[11] and recent experiments with free falling nanoparticles enable the detection of static forces,[12] the accuracy of these results does not outperform that of existing systems. In most of the levitation experiments, in fact, the uncertainties on the detected forces are of the order of few tens of percent,[12] sometimes even as high as 50%.[13] Such large errors arise from uncertainties in the particle displacement calibration,[14] whose accuracy is critically affected by the poor knowledge on the particle's mass. This results in severe limitations on their sensing and metrology applications, where the accuracy of a measurement is just as important as its precision.

Silica micro- and nanospheres are the most commonly used type of particle in levitated sensing experiments. Due to their fabrication process,[15] these particles feature a finite size distribution with a 2−5% coefficient of variation.[16] This, together with even higher uncertainties on the density of the amorphous silica used (up to 20%[17]), leads to inaccurate values of the particle's mass. One could avoid assumptions of the manufacturer specifications by relying on the kinetic theory of gases to calculate the radius of the particle.[18] Also in this case, however, the final measurement of the mass is affected by uncertainties on the material density and on other quantities, such as pressure and molar mass[19] of the surrounding media. A more accurate estimation of the particle's mass is therefore highly desirable, as it would boost the accuracy of sensors based on levitated particles.

Here, we propose and experimentally demonstrate a measurement protocol that is unaffected by the above-mentioned uncertainties (density, pressure, size, etc.) and

Received: January 8, 2019
Revised: March 4, 2019
Published: March 19, 2019

DOI: 10.1021/acs.nanolett.9b00082
Nano Lett. 2019, 19, 6711−6715

leads to an assessment of the particle's mass within 2.2% systematic error and 0.9% statistical error. Our method exploits a new design of an optical trap in which a pair of electrodes is placed around the focus and is based on the analysis of the response of a trapped charged particle to an external electric field. Careful error estimation has been carried out in order to assess the final mass uncertainty, including the treatment of possible anharmonicities in the trapping potential. The technique we propose is easy to implement in any vacuum trapping setup and improves by more than an order of magnitude the accuracy of most precision measurements.

Experimental Set-Up. The experimental setup is depicted in Figure 1a. A single silica nanoparticle ($d = 143 \pm 4$ nm in diameter; nominal value of the manufacturer) is optically trapped in vacuum with a tightly focused laser beam (wavelength $\lambda = 1064$ nm, power $P \simeq 75$ mW, $NA = 0.8$). The oscillation of the particle along the x-mode is monitored with a balanced split detection scheme that provides a signal $v(t)$ proportional to the particle displacement $x(t) = v(t)/c_{cal}$, with c_{cal} being the linear calibration factor of the detection system.[14] Along the same axis, a pair of electrodes (see Figure 1b) form a parallel plate capacitor that we use to generate an oscillating electric field $E(t) = E_0 \cos(\omega_{dr} t)$ at the particle position, which in turn induces a harmonic force $F_{el}(t)$ on the charged particle.

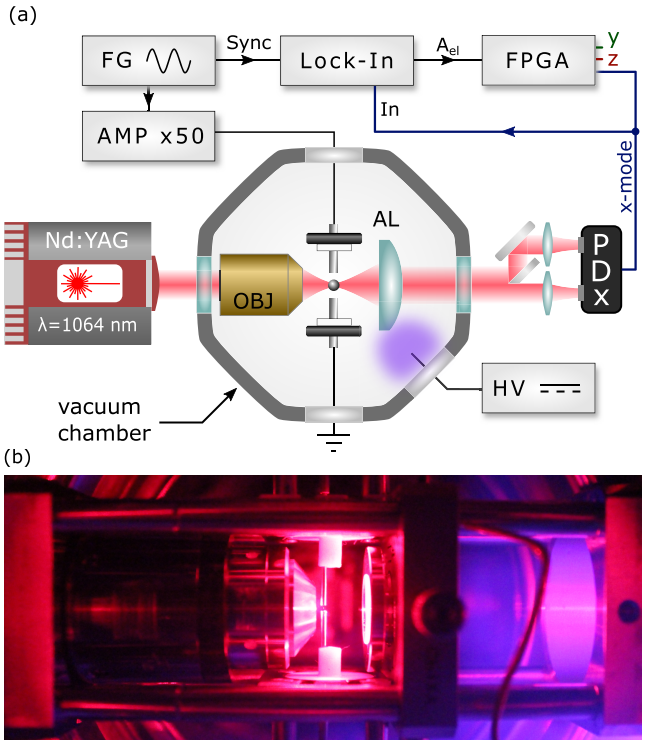

Figure 1. Experimental setup. (a) A microscope objective (OBJ) focuses a laser beam inside a vacuum chamber, where a single silica nanoparticle is trapped in the focus. The light scattered by the particle is collected with an aspheric lens (AL), and the motion of the particle is detected in a split detection scheme. A pair of electrodes is connected to the amplified signal from a function generator (FG), creating an electric field that drives the charged particle. An FPGA and a lock-in amplifier are used to bandpass and record the signal from the detector. (b) A camera image of the setup inside of the vacuum chamber. The purple glow on the side of the chamber is emitted by a generated bare electrode connected to a high voltage (HV) DC source and is used to control the net charge of the particle.

The equation of motion of the particle can be described by a thermally and harmonically driven damped resonator:

$$m\ddot{x} + m\Gamma\dot{x} + kx = F_{th}(t) + F_{el}(t) \quad (1)$$

Here, m is the mass of the particle, Γ is the damping rate and $k = m\Omega_0^2$ is the stiffness of the optical trap, with Ω_0 being the mechanical eigenfrequency of the oscillator. The first forcing term F_{th} models the random collisions with residual gas molecules in the chamber. It can be expressed as $F_{th} = \sigma\eta(t)$, where $\eta(t)$ has a Gaussian probability distribution that satisfies $\langle\eta(t)\eta(t+t')\rangle = \delta(t')$, and σ relates to the damping via the fluctuation−dissipation theorem: $\sigma = \sqrt{2k_B T m\Gamma}$, with k_B being the Boltzmann constant and T the bath temperature. The second forcing term F_{el} arises from the Coulomb interaction of the charged particle with the external electric field $E(t)$ and can be expressed as $F_{el}(t) = F_0 \cos(\omega_{dr} t)$, where $F_0 = q \cdot E_0$. The net charge $q = n_q \cdot q_e$, with q_e being the elementary charge and n_q the number of charges on the particle, can be controlled[20] by applying a high DC voltage $V_{HV} \approx \pm 1$ kV on a bare electrode placed on a side of the vacuum chamber. Via the process of corona discharge,[21] this creates a plasma consisting of a mixture of positive or negative ions (depending on the V_{HV} polarity) and electrons that can ultimately add to, or remove from, the levitated particle one single elementary charge at a time. Positive and negative ions are accelerated toward opposite directions due to the presence of the electric field from the electrode. As a result, the ratio of positive to negative charges reaching the particle is biased by the electrode polarity, thus allowing us to fully control the final charge of the particle within positive or negative values (see Supplementary Section S3). This is a significant advantage compared to other discharging techniques that rely on shining UV light on the particle,[22] where the net charge can only be diminished until reaching neutrality.

Measurement. A single nanoparticle is loaded in the trap at ambient pressure by nebulizing a solution of ethanol and monodispersed silica particles into the chamber. The pressure is then decreased down to $P \lesssim 1$ mBar where the net number of charges n_q can be set with zero uncertainty. Finally, the system is brought back up to an operating pressure of $P \simeq 50$ mBar. At this pressure the particle is in the ballistic regime, but its dynamics is still highly damped. This condition is favorable for our experiments, as the high damping reduces the contribution of anharmonicities to the dynamics of the particle,[10] allowing us to apply the fully linear harmonic oscillator model which predicts

$$S_x(\omega) = S_x^{th}(\omega) + S_x^{el}(\omega) = \frac{4k_B T\Gamma}{m[(\omega^2 - \Omega_0^2)^2 + \Gamma^2\omega^2]} + \frac{F_0^2 \tau\, \mathrm{sinc}^2[(\omega - \omega_{dr})\tau]}{m^2[(\omega^2 - \Omega_0^2)^2 + \Gamma^2\omega^2]} \quad (2)$$

Here, $S_x(\omega)$ is the single-sided power spectral density (PSD) of the thermally and harmonically driven resonator, whose dynamics $x(t)$ is being observed for a time $\mathcal{T} = 2\tau$. Note that $S_x(\omega)$ relates to the experimentally measured PSD $S_v(\omega)$ via the calibration factor c_{cal}, such that $S_v(\omega) = c_{cal}^2 \cdot S_x(\omega)$.[14]

In the absence of the electric driving, the motion of the particle in the optical trap is purely thermal, and its PSD is well

DOI: 10.1021/acs.nanolett.9b00082
Nano Lett. 2019, 19, 6711−6715

approximated by a typical Lorentzian function. From an experimental measurement of $S_v^{th}(\omega)$, we can extract the value of $S_v^{th}(\omega_{dr})$ and perform maximum likelihood estimation (MLE) to obtain the values of Ω_0 and Γ as fitting parameters. Likewise, when the coherent driving is applied to the system, we are able to determine the magnitude of the driven resonance $S_v(\omega_{dr})$ and to calculate from this measurement the solely electric contribution $S_v^{el}(\omega_{dr}) = S_v(\omega_{dr}) - S_v^{th}(\omega_{dr})$. Figure 2 exemplifies this process for $\omega_{dr}/(2\pi) = 135$ kHz

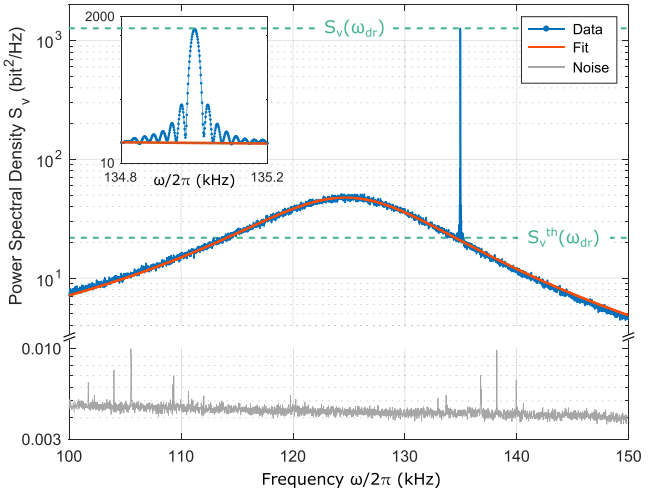

Figure 2. Measurement. Power spectral density $S_v(\omega)$ of a thermally and harmonically driven resonator at $P = 50$ mBar. The broad peak centered at $\Omega_0 \simeq 125$ kHz is the oscillator response to the thermal driving that we fit with a Lorentzian function (orange) to extract $S_v^{th}(\omega_{dr})$, together with Ω_0, Γ and the corresponding uncertainties. The narrow band peak at $\omega = 135$ kHz, also shown in detail in the inset, depicts to the electric excitation, from which we retrieve $S_v^{el}(\omega_{dr}) = S_v(\omega_{dr}) - S_v^{th}(\omega_{dr})$. The gray spectrum at the bottom of the plot is the measurement noise, which is $\gtrsim 40$ dB below the particle's signal.

and for a signal-to-noise SNR $= S_v(\omega_{dr})/S_v^{th}(\omega_{dr}) \simeq 60$. The curve shown is computed with Bartlett's method from an ensemble of $N_{psd} = 1000$ averages of individual PSDs, calculated from $\mathcal{T} = 40$ ms position time traces. In Supplementary Section S2, we verify that over the whole measurement time $t = N_{psd} \times \mathcal{T} = 40$ s the system does not suffer from low frequency drifts. The electrically driven peak can be fully resolved (see inset in Figure 2), and its shape agrees with the Fourier transform of the rectangular window function used for PSD estimation. The gray trace at the bottom of the plot represents the measurement noise, which is ~40 db below the thermal signal and more than 55 db below the driven peak. Finally, the solid line is a MLE fit of a thermally driven Lorentzian to the experimental data. Note that, to perform the fit and to retrieve the value of $S_v^{th}(\omega_{dr})$, the electrically driven peak is numerically filtered out by applying to the time series data set a notch filter of variable bandwidth b around ω_{dr}. The value of b depends on the driving amplitude, with typical values of the order of tens of Hertz. In Supplementary Section S7, we show how this method introduces negligible errors that remain always below ~0.01%.

The mass of the particle can ultimately be calculated considering the ratio $R_S = \frac{S_v^{el}(\omega_{dr})}{S_v^{th}(\omega_{dr})} = \frac{S_v - S_v^{th}}{S_v^{th}}|_{\omega=\omega_{dr}}$. In fact, note that, while both S_v^{el} and S_v^{th} depend quadratically on c_{cal}, the latter scales as m^{-1} while the former scales as m^{-2}. Thus, from their ratio we obtain

$$m = \frac{n_q^2 q_e^2 E_0^2 \mathcal{T}}{8 k_B T \Gamma R_S} \tag{3}$$

To ensure the validity of the linear resonator model, we also considered a cubic term in the restoring force and performed Monte Carlo Simulations of the resulting Duffing resonator with parameters compatible with our experimental settings and an overestimated value of the Duffing coefficient,[23,24] $\xi = 12\ \mu m^{-2}$. The outcome of the simulations is detailed in Supplementary Section S5 and confirms the negligibility of the nonlinear terms for pressures of $P \simeq 50$ mBar. We stress that this assumption fails already at slightly lower pressures of ~10 mBar where a more complicated nonlinear response model would be needed.

Error Estimation. In order to estimate the systematic error in the calculated mass, a careful study of all the sources of error has to be carried out. Table 1 summarizes the absolute values

Table 1. Uncertainties Table[a]

Quantity	Value z_i	Error σ_{z_i}/z_i
n_q	8	0
q_e	1.602×10^{-19} C	6.1×10^{-9}
E_0	5.305 kVm^{-1}	0.011
$\mathcal{T}$	40 ms	4×10^{-5}
$S_v(\omega_{dr})$	1057.8 bit^{2}Hz^{-1}	0.005
$S_v^{th}(\omega_{dr})$	14.7	0.007
k_B	1.380×10^{-23} JK^{-1}	5.72×10^{-7}
T	295.8 K	0.002
Γ	1.998×10^5 rads^{-1}	0.003
m	**4.01 fg**	**0.009** (stat.) ± **0.024** (syst.)

[a]The different quantities z_i involved in the calculation of the mass are here reported together with the corresponding error σ_{z_i}. Color coding indicates negligibility of the uncertainty, with gray rows implying $\sigma_{z_i} \simeq 0$.

and the relative uncertainties of the quantities entering in eq 3. The specific case reported corresponds to point at $\omega_{dr} = 125$ kHz of the data shown in Figure 3. For several variables and constants, we can neglect the corresponding uncertainty. Accordingly, for the error propagation we set $\sigma_{q_e} = \sigma_{\mathcal{T}} = \sigma_{k_B} = 0$. Note that the specific number of charges $n_q = 8$ chosen in our measurements is arbitrary. Other measurements have been previously carried out with different values of n_q and have confirmed the independency of the method from n_q, provided the dynamics is maintained in the linear regime of oscillation. Concerning the other quantities, instead, we follow the arguments stated below:

(i) The electric field was simulated with the finite elements method and was mainly affected by uncertainties in the geometry of the electrodes (see Supplementary Section S4 for further details). We measure a distance between electrodes of $d_{el} = 1410\ \mu m \pm 13\ \mu m$, and a corresponding electric field (for an applied dc potential of 1 V) $E_0 = 577 \pm 6$ V/m.

DOI: 10.1021/acs.nanolett.9b00082
Nano Lett. 2019, 19, 6711−6715

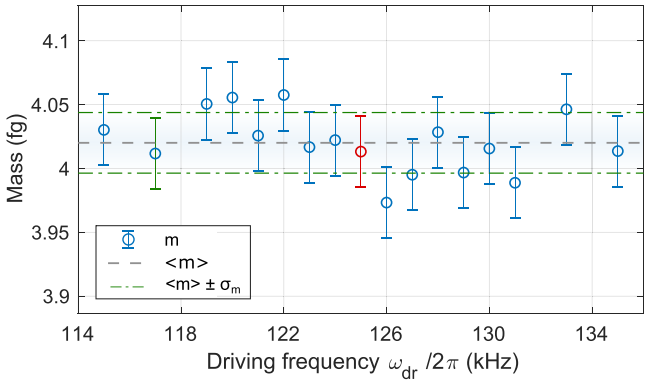

Figure 3. Results of mass calculation. The mass of the levitated nanoparticle m is calculated for different driving frequencies ω_{dr}. Error bars correspond to the statistical error σ_m^{stat}, calculated from a reproducibility measurement of 20 independent data sets of same experimental conditions: $\omega_{dr} = 125$kHz and SNR = 60. The measurement is shown to be independent from the chosen driving frequency ω_{dr}, and the standard deviation (green horizontal lines) displays compatibility with the statistical error. Values reported in Table 1 correspond the red-highlighted point at $\omega_{dr} = 125$ kHz.

(ii) The two heights of the power spectral densities $S_v(\omega_{dr})$ and $S_v^{th}(\omega_{dr})$ from which the ratio R_S is calculated are only affected by statistical errors since simulations confirm the validity of the linear model. σ_{S_v} is thus calculated from an ensemble of N_{PSD} measurements as the standard error of the mean, with the $1/\sqrt{N_{PSD}}$ trend being verified. The same applies for S_v^{th}, where in this case $\sigma_{S_v^{th}}$ is calculated in the absence of external electric driving.

(iii) The thermal bath surrounding the particle is assumed to be constantly thermalized with the setup and, more precisely, with the vacuum chamber walls. Again, the moderate-high pressure $P = 50$ mBar ensures this assumption. Multiple temperature measurements on the surface of the vacuum chamber are carried out with a precision thermistor (0.5 °C accuracy) in order to exclude the presence of temperature gradients and significant variations during the experimental times (see Supplementary Section S8 for data and further discussion).

(iv) The uncertainty of fitting parameters such as Ω_0 and Γ can be extracted directly from the Lorentzian fits.

The variables involved in eq 3 can be considered uncorrelated, and the standard uncertainty propagation[25] can be performed. A detailed derivation is provided in Supplementary Section S9.

Results. The statistical error σ_m^{stat} of our measurement is calculated from the standard deviation of a set of 20 independent measurements performed at $\omega_{dr}/2\pi = 130$ kHz and for SNR $\simeq$ 60. We find $\sigma_m^{stat}/m = 0.7\%$. This dispersion is displayed as error bars in Figure 3, where we plot the calculated mass as a function of ω_{dr}, again for SNR $\simeq$ 60. The region within green dot-dashed lines corresponds to the standard deviation $\pm\sigma_m^{sweep}$ of the presented data.

The compatibility $\sigma_m^{stat} \simeq \sigma_m^{sweep}$ and the reproducibility of the mass calculated at different driving frequencies reveal that the measurements are not affected by nonlinearities in the system. In fact, strong driving fields lead to anharmonic particle dynamics, which in turn introduce an unphysical mass dependency on ω_{dr}. Figure S6a in Supplementary Section S2 exemplifies this situation and shows how in the nonlinear regime the calculated mass is affected by severe systematic errors. In our method, we avoid this situation by maintaining the driving field amplitude below 5.5kV/m. In this regime, we have additionally verified the independency of the calculated mass from the electric field E_0 and tested the quadratic scaling of R_S as a function of E_0. These measurements are described in Figure S3 of the Supporting Information. The excellent agreement with the model provides a further validation of eq 3 and of the harmonic approximation made. As a final remark, we compare the measured mass m of a $d = 143 \pm 4$ nm diameter particle with the one calculated from the manufacturer specifications m_{man}. Assuming a nominal density for Stöber silica of $\rho_p = 2200$ kg/m^3 and propagating the corresponding uncertainties, one finds $m_{man} = (3.37 \pm 0.84)$ fg, which shows good agreement with the value measured with our method $m = (4.01 \pm 0.1)$ fg.

Conclusions. In conclusion, we presented a novel protocol to calculate the mass of a levitated nanosensor through its electrically driven dynamics. We stress that this method only assumes a driven damped harmonic oscillator. As such, it is suitable to measure the oscillator's mass in a large variety of optical trapping systems and possibly also in more general mechanical resonator schemes. The level of precision and accuracy obtained establishes an improvement of more than one order of magnitude compared to the state-of-the-art methods, enabling paramount advances in the applications of levitated systems as force sensors and accelerometers. Moreover, this technique leads to a much more reliable calibration of the particle's displacement,[14] again providing an important step for the use of levitated systems for metrology and sensing applications, and toward compliance requirements of groundbreaking experiments such as MAQRO.[26]

■ ASSOCIATED CONTENT

Supporting Information

The Supporting Information is available free of charge on the ACS Publications website at DOI: 10.1021/acs.nanolett.9b00082.

Harmonic approximation throughout studying (via both experimental data and simulations) the nonlinear dynamics of the system for high electric drivings. Stability of the system as a way to minimize the statistical error in our protocol. Simulations of the electric field and error estimations for all the variables involved in our method (with particular attention on the electric field and the bath temperature) (PDF)

■ AUTHOR INFORMATION

Corresponding Authors

*E-mail: francesco.ricci@icfo.eu.
*E-mail: romain.quidant@icfo.eu.

ORCID

F. Ricci: 0000-0002-5971-3369
G. P. Conangla: 0000-0002-3228-1527
R. Quidant: 0000-0001-8995-8976

DOI: 10.1021/acs.nanolett.9b00082
Nano Lett. 2019, 19, 6711−6715

Author Contributions

F.R. and A.S. conceived the experiment. F.R. designed and implemented the experimental setup and wrote all data acquisition software. F.R. and M.T. performed the experiment and analyzed the data, with inputs from G.P. Montecarlo and COMSOL simulations were performed by G.P. and M.T., respectively. All authors contributed to manuscript writing. R.Q. and A.S. supervised the work.

Notes

The authors declare no competing financial interest.

■ ACKNOWLEDGMENTS

We acknowledge financial support from the ERC-QnanoMECA (Grant No. 64790), the Spanish Ministry of Economy and Competitiveness, under grant FIS2016-80293-R and through the "Severo Ochoa" Programme for Centres of Excellence in R&D (SEV-2015-0522), Fundació Privada CELLEX, and from the CERCA Programme/Generalitat de Catalunya. We also acknowledge N. Meyer and the rest of the PNO trapping team. F.R. acknowledges Dr. M. Frimmer and Prof. L. Novotny from ETH (Zurich) for valuable discussions and A. Bachtold (ICFO) for providing a general perspective on the accuracy of mechanically resonating nanosensors.

■ REFERENCES

(1) Moser, J.; Güttinger, J.; Eichler, A.; Esplandiu, M. J.; Liu, D. E.; Dykman, M. I.; Bachtold, A. *Nat. Nanotechnol.* **2013**, *8*, 493.
(2) Chaste, J.; Eichler, A.; Moser, J.; Ceballos, G.; Rurali, R.; Bachtold, A. *Nat. Nanotechnol.* **2012**, *7*, 301.
(3) Cleland, A. N.; Roukes, M. L. *Nature* **1998**, *392*, 160.
(4) Yin, Z. Q.; Geraci, A. A.; Li, T. C. *Int. J. Mod. Phys. B* **2013**, *27*, 1330018.
(5) Norte, R. A.; Moura, J. P.; Gröblacher, S. *Phys. Rev. Lett.* **2016**, *116*, 147202.
(6) Purdy, T. P.; Peterson, R. W.; Yu, P.-L.; Regal, C. A. *New J. Phys.* **2012**, *14*, 115021.
(7) Gieseler, J.; Deutsch, B.; Quidant, R.; Novotny, L. *Phys. Rev. Lett.* **2012**, *109*, 1−5.
(8) Jain, V.; Gieseler, J.; Moritz, C.; Dellago, C.; Quidant, R.; Novotny, L. *Phys. Rev. Lett.* **2016**, *116*, 243601.
(9) Setter, A.; Toroš, M.; Ralph, J. F.; Ulbricht, H. *Phys. Rev. A: At., Mol., Opt. Phys.* **2018**, *97*, 033822.
(10) Gieseler, J.; Novotny, L.; Quidant, R. *Nat. Phys.* **2013**, *9*, 806−810.
(11) Ranjit, G.; Cunningham, M.; Casey, K.; Geraci, A. A. *Phys. Rev. A: At., Mol., Opt. Phys.* **2016**, *93*, 053801.
(12) Hebestreit, E.; Frimmer, M.; Reimann, R.; Novotny, L. *Phys. Rev. Lett.* **2018**, *121*, 063602.
(13) Hempston, D.; Vovrosh, J.; Toroš, M.; Winstone, G.; Rashid, M.; Ulbricht, H. *Appl. Phys. Lett.* **2017**, *111*, 133111.
(14) Hebestreit, E.; Frimmer, M.; Reimann, R.; Dellago, C.; Ricci, F.; Novotny, L. *Rev. Sci. Instrum.* **2018**, *89*, 033111.
(15) Stöber, W.; Fink, A.; Bohn, E. *J. Colloid Interface Sci.* **1968**, *26*, 62−69.
(16) microParticles GmbH. *SiO2-R Datasheet*, 2018.
(17) Parnell, S. R.; Washington, A. L.; Parnell, A. J.; Walsh, A.; Dalgliesh, R. M.; Li, F.; Hamilton, W. A.; Prevost, S.; Fairclough, J. P. A.; Pynn, R. *Soft Matter* **2016**, *12*, 4709−4714.
(18) Beresnev, S. A.; Chernyak, V. G.; Fomyagin, G. A. *J. Fluid Mech.* **1990**, *219*, 405−421.
(19) Hebestreit, E.; Reimann, R.; Frimmer, M.; Novotny, L. *Phys. Rev. A: At., Mol., Opt. Phys.* **2018**, *97*, 043803.
(20) Frimmer, M.; Luszcz, K.; Ferreiro, S.; Jain, V.; Hebestreit, E.; Novotny, L. *Phys. Rev. A: At., Mol., Opt. Phys.* **2017**, *95*, 061801.
(21) Fridman, A.; Kennedy, L. A. *Plasma Physics and Engineering*; CRC press, 2004.
(22) Moore, D. C.; Rider, A. D.; Gratta, G. *Phys. Rev. Lett.* **2014**, *113*, 1−5.
(23) Ricci, F.; Rica, R. A.; Spasenovic, M.; Gieseler, J.; Rondin, L.; Novotny, L.; Quidant, R. *Nat. Commun.* **2017**, *8*, 15141.
(24) Gieseler, J.; Spasenović, M.; Novotny, L.; Quidant, R. *Phys. Rev. Lett.* **2014**, *112*, 1−5.
(25) Ku, H. *J. Res. Natl. Bur. Stand., Sect. C* **1966**, *70C*, 263.
(26) Kaltenbaek, R.; et al. *EPJ. Quantum Technology* **2016**, *3*, 5.

DOI: 10.1021/acs.nanolett.9b00082
Nano Lett. 2019, 19, 6711−6715